Observation of two-dimensional defect surface solitons

A. Szameit,[1,*] Y. V. Kartashov,[2] M. Heinrich,[1] F. Dreisow,[1] T. Pertsch,[1] S. Nolte,[1] A. Tünnermann,[1,3] F. Lederer,[4] V. A. Vysloukh,[2] and L. Torner[2]

[1]*Institute of Applied Physics, Friedrich-Schiller-Universität Jena, Max-Wien-Platz 1, 07743 Jena, Germany*
[2]*ICFO-Institut de Ciencies Fotoniques and Universitat Politecnica de Catalunya, Mediterranean Technology Park, 08860 Castelldefels (Barcelona), Spain*
[3]*Fraunhofer Institute for Applied Optics and Precision Engineering, Albert-Einstein-Strasse 7, 07745 Jena, Germany*
[4]*Institute for Condensed Matter Theory and Optics, Friedrich-Schiller-Universität Jena, Max-Wien-Platz 1, 07743 Jena, Germany*
Corresponding author: szameit@iap.uni-jena.de

We report on the experimental observation of two-dimensional solitons located in defect channels at the surface of a hexagonal waveguide array. The threshold power for the excitation of solitons existing owing to total internal reflection grows with decrease of the refractive index in negative defects and vanishes for sufficiently strong positive defects. Negative defects can also support linear surface modes existing owing to Bragg-type reflections. © 2009 Optical Society of America

OCIS codes: 190.0190, 190.6135.

Discrete solitons [1,2] may emerge at interfaces of materials yielding different physical properties. When they form at the interface of uniform and periodic nonlinear media [3,4] they combine the characteristics of surface states at uniform interfaces and the unique properties of lattice solitons arising from the periodicity of underlying medium. Surface solitons may exist at defocusing lattice interfaces [5–7]. Recently the properties of two-dimensional surface solitons were analyzed theoretically [8–13] and experimentally [14–16]. In all these settings surface solitons were realized at the edge of perfectly periodic lattices. However, the addition of defects may substantially modify the guiding properties [17]. Lattices with defects allow for linear localized states existing owing to total internal or Bragg-type reflection [18]. When placed at the edge of a one-dimensional lattice, the defects strongly alter the properties of surface solitons [19,20]. Nevertheless, in two-dimensional structures the formation of nonlinear defect surface states and the generation of thresholdless surface waves were not observed.

In this Letter we show the existence of different types of two-dimensional defect surface solitons in hexagonal waveguide arrays, relying on different guiding mechanisms, and report on their experimental observation. We show that the threshold power and the excitation dynamics for surface solitons strongly depend on the type and strength of the surface defect.

In the simulations we employ the nonlinear Schrödinger equation for the dimensionless field amplitude q:

$$i\frac{\partial q}{\partial \xi} = -\frac{1}{2}\left(\frac{\partial^2 q}{\partial \eta^2} + \frac{\partial^2 q}{\partial \zeta^2}\right) - q|q|^2 - pR(\eta,\zeta)q. \quad (1)$$

Here ξ is the longitudinal and η, ζ are the transverse coordinates, while p stands for the refractive index modulation depth ($p=p_d$ in the defect sites, $p=p_a$ in

the rest of the array). The function $R(\eta,\zeta)$ describes the refractive index profile as a superposition of Gaussian functions $\exp[-(\eta/w_\eta)^2-(\zeta/w_\zeta)^2]$ modeling the individual waveguides, which are arranged in a hexagonal array with spacing w_s. Defect waveguides are located in the first row. We set $w_\eta=0.45$, $w_\zeta=0.9$, and $w_s=4$ in accordance with the transverse waveguide dimensions of 4.5 μm × 9 μm and the spacing of 40 μm. We fixed $p_a=2.8$ that corresponds to a real modulation depth ~3×10^{-4}. In simulations we model the array with a finite number of waveguides (according to the experiment), but results hold true for semi-infinite arrays.

The stationary profiles of defect surface solitons are of the form $q=w(\eta,\zeta)\exp(ib\xi)$, where b is the propagation constant. Such solitons exist for b values above a cutoff b_{co} and carry total power $U = \iint_{-\infty}^{\infty} w^2 d\eta d\zeta$. We found two types of defect surface states: those mediated by total internal reflection and those emerging from Bragg reflection. The states forming owing to total internal reflection never change their sign between the waveguides [Figs. 1(a)–1(c)]. Their properties are summarized in Figs. 2(a)–2(c). When $p_d \leqslant 2.94$ the $U(b)$ dependence for surface solitons is nonmonotonic [Fig. 2(a), curve 1]. Solitons exist only above the power threshold U_{th}. The slope of $U(b)$ curve tends to infinity in the cutoff, where the soliton is most extended. Also, U_{th} increases with decreasing p_d [Fig. 2(b)], while the cutoff changes only slightly. In contrast, for $p_d > 2.94$ the cutoff changes rapidly [Fig. 2(c)] while U_{th} vanishes [Fig. 2(a), curves 2 and 3], since strong positive surface defects support linear modes [shapes of low-power solitons close to linear modes are shown in Figs. 1(a) and 1(c)]. Note that for $p_d \approx 2.94$, when the penetration of the field into the lattice is maximal, increasing or decreasing the defect strength results in a dramatic reduction of the light field penetration, even close to the cutoff. Far from the cutoff the light
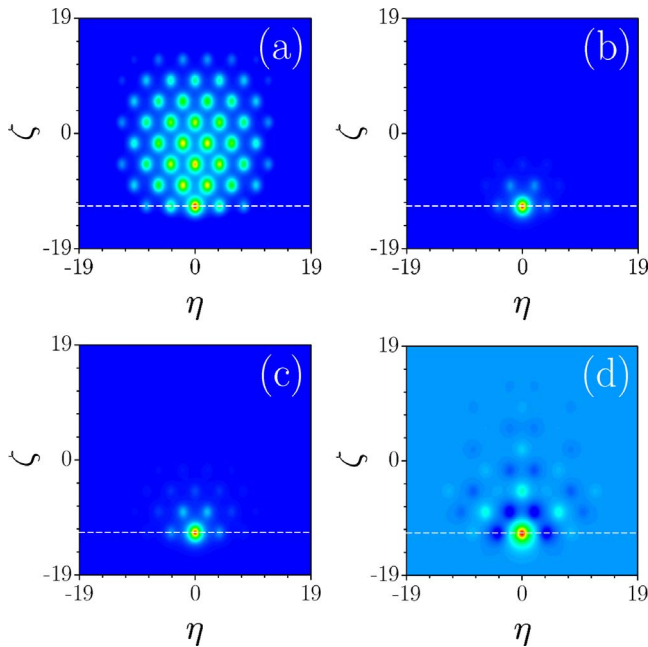
Fig. 1. (Color online) Field distributions for defect surface solitons at (a) $b=0.4644$, $p_d=2.96$; (b) $b=0.512$, $p_d=2.96$; (c) $b=0.49$, $p_d=3.1$; (d) $b=0.274$, $p_d=1.7$. The white dashed lines indicate the interface position.

gradually concentrates in the defect site [Fig. 1(b)]. Since only states on the $dU/db > 0$ branches of the $U(b)$ curve are linearly stable, there exist narrow instability domains close to the cutoff for $2.94 < p_d < 2.99$. For $p_d > 2.99$ the surface solitons become stable in the entire domain of existence.

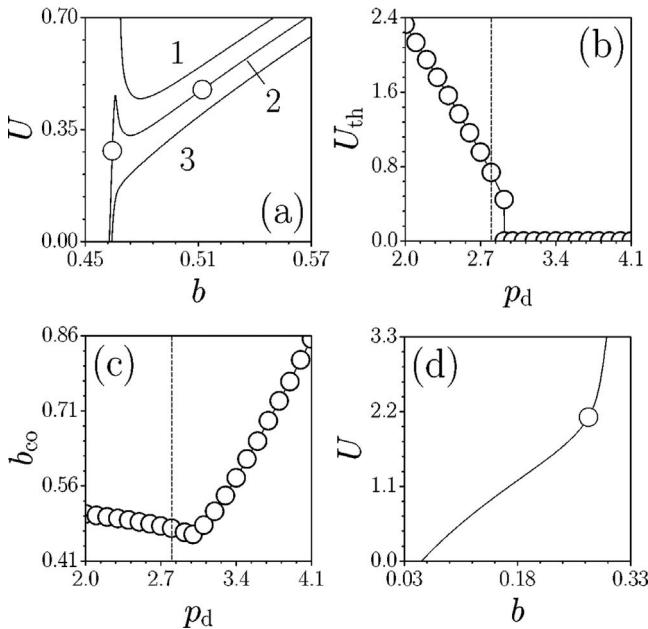Negative defects ($p_d < 2.8$) may support a second type of surface modes mediated by Bragg-type reflec-

Fig. 2. (a) Power versus propagation constant for $p_d = 2.92$ (curve 1), 2.96 (curve 2), and 3 (curve 3). The circles correspond to solitons in Figs. 1(a) and 1(b). (b) Threshold power and (c) cutoff versus p_d. Dashed lines indicate the point $p_d = 2.8$. (d) Power versus propagation constant for a surface mode existing owing to Bragg guiding at $p_d = 1.7$. The circle corresponds to profile from Fig. 1(d).

tion from the periodic structure. The field of such modes exhibits a complicated staggered structure [Fig. 1(d)]. Nonlinear surface modes supported by negative defects bifurcate from such linear surface modes; hence their power vanishes in the cutoff [Fig. 2(d)]. Therefore, such states can be excited with very small powers. This is in sharp contrast to defect surface solitons mediated by total internal reflection, which feature considerable thresholds at such small p_d values. The degree of localization of staggered surface modes increases, and their narrow domain of existence expands with decreasing p_d.

For the experimental observation of defect surface solitons we used waveguide arrays in fused silica glass fabricated with a femtosecond direct writing technique [21]. The length of our samples was 105 mm, while the spacing of the guides was 40 μm. The writing velocity was 1750 μm/s to keep the uniform nonlinear refractive index of the unprocessed material in the waveguides [22]. The defect sites were written with 1500 and 2000 μm/s for a positive defect and negative defect, respectively. For the excitation of the solitons, we used a 1 kHz fs laser system (Spectra Tsunami/Spitfire) with a pulse length of about 180 fs at a central wavelength of 800 nm. To confirm the experimental data by simulations, we solved Eq. (1) with the input conditions $q|_{\xi=0} = A \exp[-(\eta - \eta_d)^2 - (\zeta - \zeta_d)^2]$, where η_d, ζ_d are the coordinates of the center of the defect surface waveguide. Note that our experiments are conducted with pulsed pump light, while the numerical simulations assume cw illumination; thus the comparison serves only to confirm the consistency of observations with soliton formation around the pulse peak.

In the array without defect (Fig. 3) the formation of nonlinear surface waves is similar to that in recent experiments [23]. At low powers one observes strong linear diffraction [Fig. 3(a)]. For intermediate power levels, the light gradually contracts toward the excited surface channel [Fig. 3(b)]. The formation of surface soliton is observed above the threshold power [Fig. 3(c)]. The picture changes dramatically in the case of a positive surface defect. Stronger defects re-
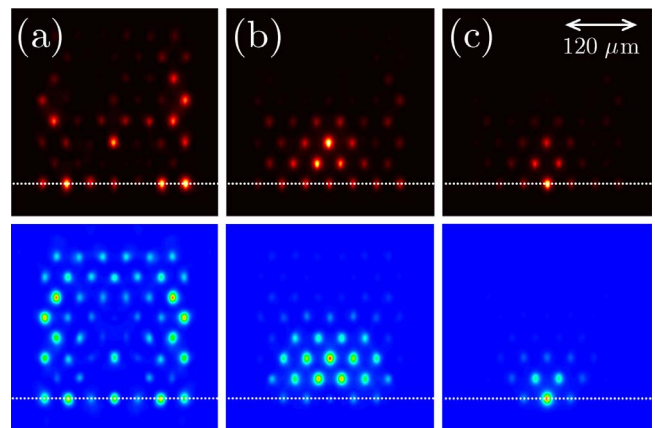

Fig. 3. (Color online) Comparison of the output intensity distributions for an excitation of a surface waveguide in array without defect at $p_d = p_a = 2.8$. Top row, experiment; bottom row, theory. The input peak power is (a) 0.18 MW, (b) 1.3 MW, and (c) 3.2 MW.
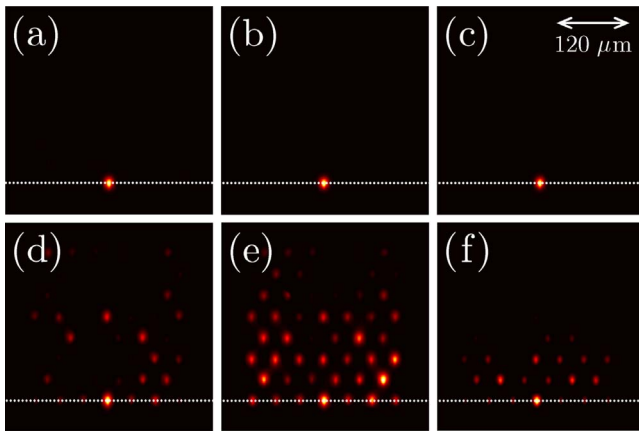
Fig. 4. (Color online) Output intensity distributions for an excitation of (a)–(c) positive surface defect waveguide at p_d=3.03, p_a=2.8 or (d)–(f) negative surface defect waveguide at p_d=2.7, p_a=2.8. Input peak power is (a) 0.2 MW, (b) 1.3 MW, (c) 2.7 MW, (d) 0.2 MW, (e) 1.3 MW, and (f) 3.2 MW.

sult in a gradual suppression of light diffraction even at low powers and, eventually, in the formation of a linear surface mode. This is accompanied by a strong reduction of the power threshold for soliton excitation. Thus an array with a strong positive defect (p_d=3.03) supports a well-localized linear mode shown in Fig. 4(a). At all power levels the light remains confined to the surface defect waveguide. An increase of the input power does not result in considerable changes of the mode profiles [see Figs. 4(b) and 4(c)].

We also observed light localization at low powers in the case of a negative surface defect for p_d=2.7 [Fig. 4(d)], a result that we attribute to the existence of linear defect caused by Bragg-type reflection from the periodic structure. Notice that in the absence of defects surface modes, soliton excitation always occurs above a threshold power, for both total internal or Bragg reflection mechanisms of localization. Increasing the input power results in a matching of the total refractive index in the defect waveguide and in the array, which is accompanied by a sudden delocalization at intermediate power levels [Fig. 4(e)]. When the input power is further increased one excites the usual surface soliton existing owing to total internal reflection [Fig. 4(f)]. The threshold power for the excitation of such solitons is much higher than in the case of defect-free arrays or positive surface defects.

In conclusion, we reported on the existence of two-dimensional defect surface solitons for both positive and negative defects. The inclusion of positive defects allows for the formation of surface solitons existing owing to total internal reflection at a reduced threshold power. Negative defects may support surface states mediated by both total internal reflection and Bragg-type reflection from the periodic structure.

References

1. D. N. Christodoulides and R. I. Joseph, Opt. Lett. **13**, 794 (1988).
2. J. W. Fleischer, M. Segev, N. K. Efremidis, and D. N. Christodoulides, Nature **422**, 147 (2003).
3. K. G. Makris, S. Suntsov, D. N. Christodoulides, G. I. Stegeman, and A. Hache, Opt. Lett. **30**, 2466 (2005).
4. S. Suntsov, K. G. Makris, D. N. Christodoulides, G. I. Stegeman, A. Haché, R. Morandotti, H. Yang, G. Salamo, and M. Sorel, Phys. Rev. Lett. **96**, 063901 (2006).
5. Y. V. Kartashov, V. A. Vysloukh, and L. Torner, Phys. Rev. Lett. **96**, 073901 (2006).
6. C. R. Rosberg, D. N. Neshev, W. Krolikowski, A. Mitchell, R. A. Vicencio, M. I. Molina, and Y. S. Kivshar, Phys. Rev. Lett. **97**, 083901 (2006).
7. E. Smirnov, M. Stepic, C. E. Rüter, D. Kip, and V. Shandarov, Opt. Lett. **31**, 2338 (2006).
8. Y. V. Kartashov and L. Torner, Opt. Lett. **31**, 2172 (2006).
9. Y. V. Kartashov, A. A. Egorov, V. A. Vysloukh, and L. Torner, Opt. Express **14**, 4049 (2006).
10. K. G. Makris, J. Hudock, D. N. Christodoulides, G. I. Stegeman, O. Manela, and M. Segev, Opt. Lett. **31**, 2774 (2006).
11. Y. V. Kartashov, V. A. Vysloukh, D. Mihalache, and L. Torner, Opt. Lett. **31**, 2329 (2006).
12. R. A. Vicencio, S. Flach, M. I. Molina, and Y. S. Kivshar, Phys. Lett. A **364**, 274 (2007).
13. H. Susanto, P. G. Kevrekidis, B. A. Malomed, R. Carretero-Gonzalez, and D. J. Frantzeskakis, Phys. Rev. E **75**, 056605 (2007).
14. X. Wang, A. Bezryadina, Z. Chen, K. G. Makris, D. N. Christodoulides, and G. I. Stegeman, Phys. Rev. Lett. **98**, 123903 (2007).
15. A. Szameit, Y. V. Kartashov, F. Dreisow, T. Pertsch, S. Nolte, A. Tünnermann, and L. Torner, Phys. Rev. Lett. **98**, 173903 (2007).
16. A. Szameit, Y. V. Kartashov, F. Dreisow, M. Heinrich, V. Vysloukh, T. Pertsch, S. Nolte, A. Tünnermann, F. Lederer, and L. Torner, Opt. Lett. **33**, 663 (2008).
17. Z. Chen, invited talk at the 407 Heraeus Workshop "Discrete Optics and Beyond," Bad Honnef, Germany, May 19–21, 2008.
18. I. Makasyuk, Z. Chen, and J. Yang, Phys. Rev. Lett. **96**, 223903 (2006).
19. M. I. Molina, I. L. Garanovich, A. A. Sukhorukov, and Y. S. Kivshar, Opt. Lett. **31**, 2332 (2006).
20. A. A. Sukhorukov, D. N. Neshev, A. Dreischuh, R. Fischer, S. Ha, W. Krolikowski, J. Bolger, A. Mitchell, B. J. Eggleton, and Y. S. Kivshar, Opt. Express **14**, 11265 (2006).
21. A. Szameit, F. Dreisow, T. Pertsch, S. Nolte, and A. Tünnermann, Opt. Express **15**, 1579 (2007).
22. D. Blömer, A. Szameit, F. Dreisow, J. Burghoff, T. Schreiber, T. Pertsch, S. Nolte, F. Lederer, and A. Tünnermann, Opt. Express **14**, 2151 (2006).
23. A. Szameit, Y. V. Kartashov, V. A. Vysloukh, M. Heinrich, F. Dreisow, T. Pertsch, S. Nolte, A. Tünnermann, F. Lederer, and L. Torner, Opt. Lett. **33**, 1542 (2008).